

Cluster–Void Degeneracy Breaking: Modified Gravity in the Balance

Martin Sahlén^{1,2*} and Joseph Silk^{2,3,4,5}

*Department of Physics and Astronomy, Uppsala University, SE-751 20 Uppsala, Sweden¹
The Johns Hopkins University, Department of Physics & Astronomy, 3400 N. Charles St., Baltimore, MD 21218, USA²
Institut d'Astrophysique de Paris, 98 bis bd Arago, F-75014 Paris, France³
AIM-Paris-Saclay, CEA/DSM/IRFU, CNRS, Univ Paris 7, F-91191, Gif-sur-Yvette, France⁴
BIPAC, University of Oxford, 1 Keble Road, Oxford OX1 3RH, UK⁵*

Combining galaxy cluster and void abundances is a novel, powerful way to constrain deviations from General Relativity and the Λ CDM model. For a flat w CDM model with growth of large-scale structure parameterized by the growth index γ of linear matter perturbations, combining void and cluster abundances in future surveys with *Euclid* and the 4-metre Multi-Object Spectroscopic Telescope (4MOST) could improve the Figure of Merit for (w, γ) by a factor of three or more compared to individual abundances. In an ideal case, the improvement on current cosmological data is a Figure of Merit factor 130.

INTRODUCTION Clusters and voids in the galaxy distribution are rare extremes of the cosmic web. Since they are sensitive probes of the statistics of the matter distribution, they can be used to place constraints on cosmological models. The abundances of clusters and voids are sensitive probes of dark energy [3, 4], modified gravity [4, 5], neutrino properties [6, 7], and non-Gaussianity [8].

In earlier work [9], we derived the first statistically significant cosmological constraints from voids, showing that the joint existence of the largest known cluster and void strongly requires dark energy in the flat Λ CDM model. We also reported a powerful parameter complementarity between clusters and voids in the Λ CDM model. Here, we extend the modelling to the case where the dark energy equation of state and matter perturbation growth index are independent, free parameters. We investigate the complementarity between cluster and void abundances for constraining deviations from the General Relativity (GR)+ Λ CDM model, and forecast ideal-case, prior-free constraints from future surveys.

FIDUCIAL SURVEYS We consider the *Euclid* Wide Survey [10] and the 4-metre Multi-Object Spectroscopic Telescope (4MOST) Galaxy Redshift Survey [11]. Survey specifications are listed in Table I. For voids, we limit ourselves to the spectroscopic segment of *Euclid* and the 4MOST spectroscopic survey, for which observational systematics should be relatively minimal (photometric redshifts can significantly distort the void shapes). We note that there is also a 4MOST cluster survey planned, which we do not consider here; our aim is to highlight the complementarity of clusters and voids, and of *Euclid* and 4MOST for void surveys.

TABLE I: Fiducial survey specifications.

| Survey | Area [sq. deg.] | Redshift |
|------------------------|-----------------|-----------|
| <i>Euclid</i> Clusters | 15000 | 0.2 – 2.0 |
| <i>Euclid</i> Voids | 15000 | 0.7 – 2.0 |
| 4MOST Voids | 12000 | 0.05 – 1 |

Cluster Selection and Limiting Cluster Mass The limiting cluster mass is chosen as $M_{200,c} = 8 \times 10^{13} h^{-1} M_{\odot}$ (where $M_{200,c}$ is the halo mass as defined by an overdensity

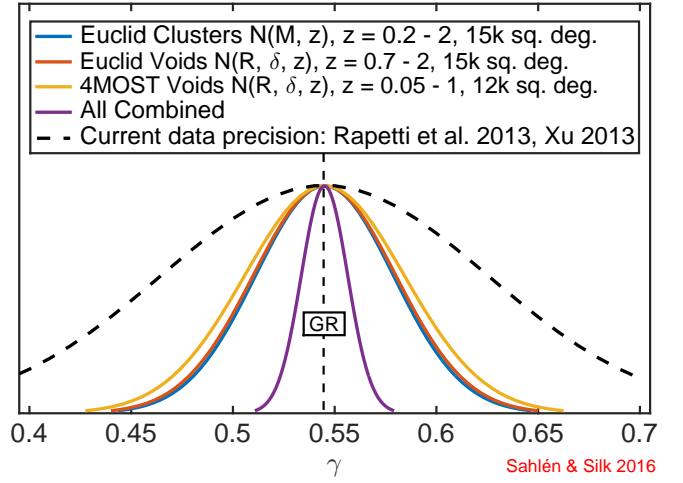


FIG. 1: Forecast marginalized pdfs for the growth index γ from cluster and void abundances in *Euclid* and 4MOST surveys, for a flat w CDM model with separate growth index γ . Note that the *Euclid* Clusters and *Euclid* Voids curves are almost identical. A pdf representative of current data precision [1, 2] is included as a dashed line. The fiducial value of $\gamma = 0.545$ for GR+ Λ CDM is also indicated.

of 200 above the critical density), with a constant 80% completeness [12]. A constant completeness level is not exact, but sufficiently accurate for our forecasting purposes.

Void Selection and Limiting Void Radius We assume that void selection is complete for voids above the limiting radius R_{lim} (with radii defined in the galaxy field). The limiting radius is set by demanding that the void radius $R > 2R_{\text{mps}} = 2\bar{n}_{\text{gal}}^{-1/3}(z)$ [3], where $\bar{n}_{\text{gal}}(z)$ is the mean comoving galaxy number density.

We use the following prescription for *Euclid*, which provides a good fit to the galaxy densities in [13]:

$$\frac{R_{\text{lim}}(z)}{h^{-1}\text{Mpc}} = 118.272 - 334.64z + 399.22z^2 - 207.26z^3 + 40.838z^4. \quad (1)$$

For 4MOST, we assume that

$$\frac{R_{\text{lim}}(z)}{h^{-1}\text{Mpc}} = \begin{cases} 13, & 0.05 \leq z \leq 0.5 \\ 31, & 0.5 < z \leq 0.7 \\ 15, & 0.7 < z \leq 0.8 \\ 17, & 0.8 < z \leq 0.9 \\ 42, & 0.9 < z \leq 1.0 \end{cases}, \quad (2)$$

based on the current survey plans [14].

Binning We use bins in redshift $\Delta z = 0.1$, cluster mass $\Delta \log(M_{200}) = 0.2$, void radius $\Delta \log(R) = 0.1$, and void density contrast $\Delta \delta_{\text{dm}} = 0.3$ (from -1 up). This binning should accommodate expected measurement uncertainties.

MODEL We predict cluster and void abundances adopting models and methodology developed in earlier work [9, 15].

Cosmological Model We assume a flat w CDM background evolution. The primordial density perturbations follow a power-law power spectrum, and neutrinos are massless. The linear growth of perturbations is determined by the growth index γ , with the linear growth rate given by [16]

$$f \equiv \frac{d \ln \delta}{d \ln a} = \Omega_m^\gamma(a). \quad (3)$$

The model is specified by today's values of the Hubble parameter h , mean matter density Ω_m , dark energy equation of state w , mean baryonic matter density Ω_b , statistical spread of the matter field at quasi-linear scales σ_8 , scalar spectral index n_s , and growth index γ .

Number Count Model We model cluster and void number counts as in [9], but with the growth of linear perturbations described by growth index γ , and background by a flat w CDM model with a constant dark-energy equation of state w .

The abundance model is given by

$$\bar{N} = \int \int \int p(O|O_t) n[M(O_t), z] \frac{dM}{dO_t} \frac{dV}{dz} dz dO_t dO, \quad (4)$$

where O is the observable (mass, radius) for clusters or voids, O_t the true physical value of the observable O , and $M(O_t)$ the (unbiased) mass estimate of the object. The differential number density is $n(M, z)$, $p(O|O_t)$ is the pdf of assigning an observed value O for a true value O_t , and dV/dz is the cosmic volume element. For integrating Eq. (4), we use $M_{\text{void}} = \frac{4}{3}\pi R^3 \rho_m(1 + \delta_{\text{dm}})$.

Number Density The differential number density of objects in a mass interval dM about M at redshift z is

$$n(M, z) dM = -F(\sigma, z) \frac{\rho_m(z)}{M\sigma(M, z)} \frac{d\sigma(M, z)}{dM} dM, \quad (5)$$

where $\sigma(M, z)$ is the dispersion of the density field at some comoving scale $R_L = (3M/4\pi\rho_m)^{1/3}$, and $\rho_m(z) = \rho_m(z = 0)(1 + z)^3$ the matter density. The expression can be written in terms of linear-theory radius R_L for voids. The multiplicity function (MF) denoted $F(\sigma, z)$ is described in the following for clusters and voids.

Cluster MF The cluster (halo) MF $F_h(\sigma)$ encodes halo collapse statistics. We use the MF of Watson et al. [17], their Eqs. (12)-(15). Mass conversions are performed using the methods in [18, Appendix C].

Void MF We employ the simulation-calibrated void MF in [3] based on a Sheth-van de Weygaert form [19], for which a critical density threshold $\delta_v = -0.43$ was derived for shell-crossed voids. We generalize this prescription to other density contrasts by computing a corresponding effective bias $b_{\text{eff}} \approx 2.45$ relative to the dark-matter density contrast at shell crossing $\delta_{\text{dm}} = -0.8$, assuming a spherical-expansion relationship [20]

$$\delta_v = c[1 - (1 + b_{\text{eff}}^{-1}\delta_{\text{dm}})^{-1/c}], \quad (6)$$

where $c = 1.594$. We then use this same relationship for other values of the dark-matter density contrast δ_{dm} , to convert to a linear density contrast δ_v to be used as the corresponding density threshold in the void MF. The void MF for (non-linear) radius R is evaluated at corresponding linear radius R_L , which here is related as $R/R_L = (1 + \delta_{\text{dm}})^{-1/3}$. Note that these spherical-expansion dynamics do not include any dark-energy or modified-gravity effects, but such corrections are sub-dominant for the model we consider [20]. We find that void-in-cloud corrections [19] are negligible for our analysis.

While our prescription for generalizing the void MF to general density contrasts should in principle be calibrated with full simulations of the galaxy field, it is robust with respect to our conclusions (for example, we have tested the effect of varying the value of the bias, and of a bias defined on the linear density field).

Scatter We include scatter in cluster and void properties as log-normal pdfs $p(O|O_t)$ for the observable O (i.e. M_{200} or R) given its true value O_t . The intrinsic scatter between observed and true cluster mass is given by [12]

$$\sigma_{\ln M(z)}^2 = \sigma_{\ln M,0}^2 - 1 + (1 + z)^{2\beta} \quad (7)$$

with $\sigma_{\ln M,0}^2 = 0.2$, $\beta = 0.125$, based on N -body simulation results. The intrinsic scatter between observed and true (spherical-equivalent) void radius is not well-studied. We assume that

$$\sigma_{\ln R(z)}^2 = \sigma_{\ln R,0}^2 \quad (8)$$

with $\sigma_{\ln R,0}^2 = 0.2$, which is a reasonable first approximation given that e.g. ellipticity varies but typically is of the order 15% [21].

Fiducial Parameters We assume $h = 0.7$, $\Omega_m = 0.3$, $\Omega_b = 0.045$, $\sigma_8 = 0.8$, $w = -1$, $n_s = 0.96$, $\Sigma m_\nu = 0 \text{ eV}$, and three neutrino species so that the early-universe effective relativistic degrees of freedom $N_{\text{eff}} = 3.046$.

LIKELIHOOD We model the number counts of clusters and voids as Poisson-distributed in each bin, and bins to be statistically independent. Hence, the log-likelihood is

$$\ln \mathcal{L} = \sum_i N_i \ln \bar{N}_i - \bar{N}_i, \quad (9)$$

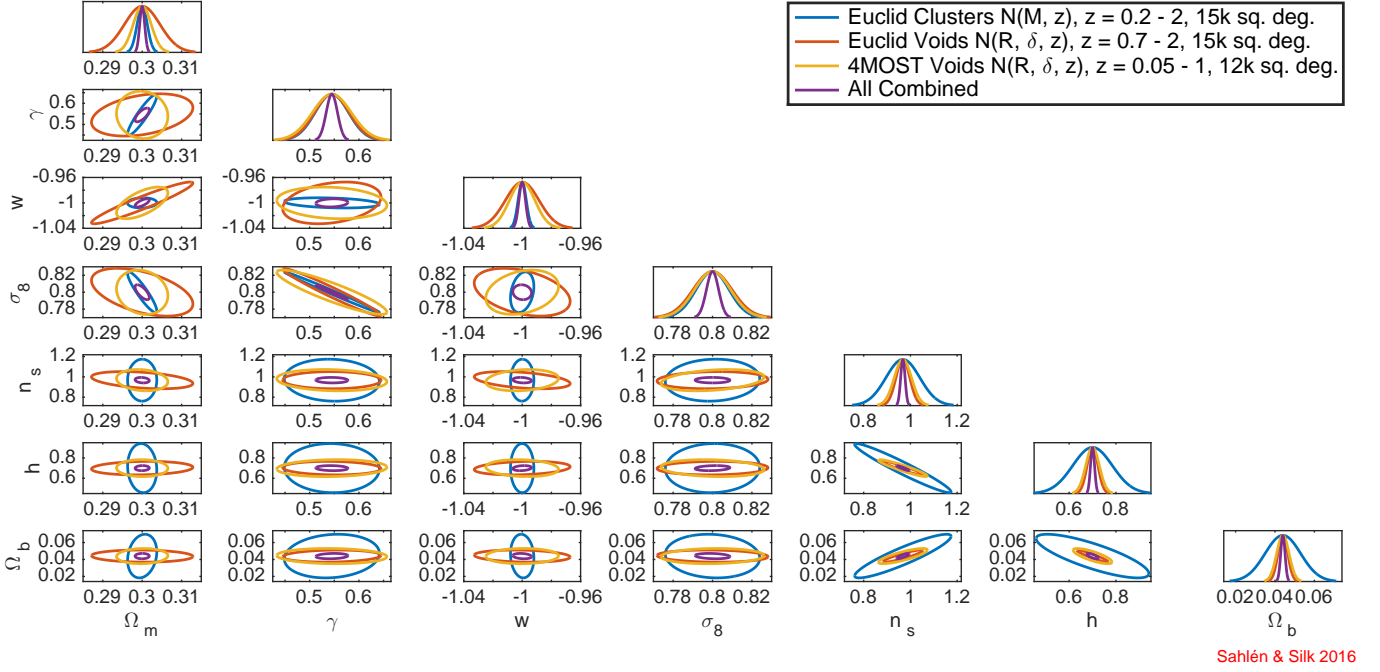


FIG. 2: Forecast 68% parameter contours, and marginal pdfs, from cluster and void abundances in future *Euclid* and 4MOST surveys, for a flat w CDM model with separate growth index γ .

where N_i is the observed number of objects in bin i , and \bar{N}_i is the model prediction, Eq. (4), for the expected number of objects in the same bin.

COMPUTATION We compute a Fisher matrix estimate of expected parameter constraints based on the Poisson likelihood [3]. This leads to a Fisher matrix

$$\mathcal{F}_{mn} = \sum_i \frac{1}{\bar{N}_i} \frac{\partial \bar{N}_i}{\partial \theta_m} \frac{\partial \bar{N}_i}{\partial \theta_n}, \quad (10)$$

where \bar{N}_i is the fiducial expected number of objects in bin i and θ_m are the different model parameters under consideration. The corresponding covariance matrix $\mathcal{C} = \mathcal{F}^{-1}$. The space of 7 free parameters is defined by $\{\Omega_m, \gamma, w, \sigma_8, n_s, h, \Omega_b\}$.

Background evolution and linear power spectrum computations are performed using a modified version of CAMB [22].

TABLE II: Forecast and current parameter uncertainties.

| Data set | $\sigma(\Omega_m)$ | $\sigma(\gamma)$ | $\sigma(w)$ | $\sigma(\sigma_8)$ | $\sigma(n_s)$ | $\sigma(h)$ | $\sigma(\Omega_b)$ |
|-----------------------------|--------------------|------------------|-------------|--------------------|---------------|-------------|--------------------|
| <i>Euclid</i> Clusters | 0.001 | 0.03 | 0.003 | 0.008 | 0.07 | 0.08 | 0.009 |
| <i>Euclid</i> Voids | 0.005 | 0.04 | 0.01 | 0.01 | 0.03 | 0.02 | 0.003 |
| 4MOST Voids | 0.002 | 0.04 | 0.01 | 0.01 | 0.04 | 0.03 | 0.003 |
| <i>Euclid</i> + 4MOST Voids | 0.002 | 0.02 | 0.005 | 0.005 | 0.02 | 0.02 | 0.002 |
| All Combined | 0.0006 | 0.01 | 0.002 | 0.003 | 0.01 | 0.01 | 0.001 |
| Current [1, 2] | 0.01 | 0.08 | 0.05 | 0.02 | 0.006 | 0.01 | 0.002 |

TABLE III: Forecast and current Figures of Merit (FoM) for the dark-energy and modified-gravity parameters w and γ .

| Data set | FoM (w, γ) |
|-----------------------------|---------------------|
| <i>Euclid</i> Clusters | 1.1×10^4 |
| <i>Euclid</i> Voids | 2.6×10^3 |
| 4MOST Voids | 3.0×10^3 |
| <i>Euclid</i> + 4MOST Voids | 1.1×10^4 |
| All Combined | 3.9×10^4 |
| Current [1, 2] | ~ 300 |

RESULTS Expected Numbers We predict 5×10^5 clusters and 9×10^5 voids in the *Euclid* cluster and void surveys, and 4×10^5 voids in the 4MOST void survey. These numbers are consistent with earlier predictions [3, 12].

Parameter Constraints The forecast ideal-case parameter constraints are shown in Fig. 1 (marginalized constraints on γ) and Fig. 2 (complete set of 1-D and 2-D pdfs) for the separate data sets and combinations thereof. Table II lists the forecast marginalized parameter uncertainties. In this ideal scenario, all surveys can improve substantially on current parameter uncertainties except for h , Ω_b and n_s . Hence, including data more informative on these parameters (e.g. cosmic microwave background data) will be a valuable, but here not crucial, addition.

Figures of Merit The Figures of Merit (FoM) for the dark-

energy and modified-gravity parameters (w, γ), defined by

$$\text{FoM} = \frac{1}{\sqrt{\det \text{cov}(w, \gamma)}}, \quad (11)$$

are listed in Table III. Compared to current data, an improvement factor 130 is expected in this ideal case. The *Euclid* cluster survey is equally informative as are the combined *Euclid*+4MOST void surveys, with a factor $\sim 3 - 4$ improvement when all are combined. With more detailed modelling of the galaxy cluster and void distributions including mass-observable scaling relations and other sources of uncertainty, the relative improvement can be expected to be greater, since such physics and systematics are mostly independent between clusters and voids. The details of this, particularly for voids, is the subject for ongoing work in the field.

Parameter Sensitivity Cluster and void number count parameter constraints are complementary for a number of different parameters. The parameters w and γ are here weakly correlated. For the individual surveys, the Pearson correlation coefficient is $\rho \sim -0.28$ to 0.28 . For the combined *Euclid* + 4MOST void surveys, $\rho = -0.09$, and for all surveys combined $\rho = 0.13$. For current data constraints, $\rho \sim -0.6$ [1, 2].

Complementary degeneracies between σ_8 , γ , Ω_m and w arise because clusters and voids have different redshift sensitivity to structure growth vs. volume expansion, and orthogonal sensitivities between matter dispersion σ and Ω_m [9, Section 4.5]. This explains why *Euclid* and 4MOST constraints are complementary in the same parameters, due to different redshift coverage (despite the *Euclid* void sample being twice as large).

For parameters describing the *shape* of the matter power spectrum (n_s, h, Ω_b) the degeneracies are orthogonal between clusters and voids. This is a reflection of orthogonal sensitivity between matter dispersion σ and Ω_m .

The results are consistent with the finding that most voids in the Baryon Oscillation Spectroscopic Survey (BOSS) have a density contrast minimum between -0.9 and -0.6 , and radius between 20 and $40 h^{-1}$ Mpc [23]. Voids that fall outside these ranges are relatively rare, with great statistical weight. Consequently, the intermediate density-contrast bin adds relatively little constraining power compared to the deep and shallow bins. The BOSS analysis, finding a 3σ discrepancy in the number of deep voids relative to the simplest allowed Λ CDM model, also independently hints that the void density-contrast distribution contains novel cosmological information.

The distribution of shallow voids is insensitive to non-linear evolution, so power spectrum and linear growth determines their size. Therefore, degeneracies between Ω_m , w and γ are almost orthogonal comparing shallow and deep voids. Shallow voids also exhibit very weak degeneracy between γ and power spectrum parameters. Further, most deep voids are large whereas shallow voids are smaller, so they probe different scales in the matter power spectrum. This produces complementary degeneracy directions between the power spectrum parameters to produce tight joint constraints when shallow and deep voids are combined.

Systematics We do not explicitly marginalize over any systematics, but have included a net effect on number counts through statistical scatter in cluster masses and void radii. The value of this scatter is assumed to be known in the forecasts, since our purpose is to establish an ideal-case limit. In the case of voids, the expected value of this scatter is not well-known, but we consider only spectroscopic data to limit photometric shape distortions. It could arise due to e.g. intrinsic ellipticity, projection and Alcock–Paczynski effects, and redshift-space distortion. We also expect linear voids to have more irregular shapes than non-linear voids, so scatter should vary with density contrast and redshift. The impact of these effects is a subject for further study; some also contain additional cosmological information.

Our void MF is a rough approximation, suited to this proof of concept. Accurate theoretical predictions based on large-scale simulations including non-linear modified gravity effects, detailed void characteristics, selection methods, and survey specifications are required for detailed forecasts and future real analyses. The detailed completeness in R and δ , and sources of bias such as survey boundary effects [23, 24], all require further study.

Cluster samples can suffer bias due to poor mass calibration and scaling relations, skewed redshift estimates, poorly understood selection, or MF modelling, but these issues are not expected to prevent percent-level cluster cosmology with e.g. *Euclid* [12].

Ultimately, combining clusters and voids (in conjunction also with e.g. cosmic microwave background data) will help limit the impact of systematics since they, as shown here, are relatively independent probes.

CONCLUSION Combining parameter constraints from cluster and void abundances in future surveys could ideally constrain deviations from GR+ Λ CDM on cosmological scales to percent level. The combination can improve the dark-energy/modified-gravity Figure of Merit a factor of three or more relative to individual abundances, and ideally a factor 130 relative to current cosmological data. This is due to clusters and voids having complementary redshift sensitivity to growth of structure vs. volume expansion, and voids probing the matter power spectrum more directly and across a wider range of scales than clusters do. This statistical power is independent of data from the cosmic microwave background, and hence can provide a precise and independent late-Universe probe of the power spectrum of density fluctuations (but cosmic microwave background data will improve constraints).

Including additional statistics (e.g. correlation functions) and properties (e.g. measurements of cluster masses, void/cluster density profiles, gravitational lensing, ellipticities) of the void and cluster distributions should improve on this significantly. The ongoing development of void cosmology carries great potential to provide added value to current and future large-area surveys for constraining deviations from the cosmological concordance model, at low or no additional cost.

ACKNOWLEDGMENTS We thank Tom Kitching, Brice

Ménard and Johan Richard for helpful input. MS thanks the Department of Physics & Astronomy at the Johns Hopkins University for hospitality during the preparation of this work. MS was supported by the Olle Engkvist Foundation (Stiftelsen Olle Engkvist Byggmästare), the US-Sweden Fulbright Commission, the Helge Ax:son Johnson Foundation (Helge Ax:son Johnsons stiftelse), and the Längmanska Fund for Culture (Längmanska kulturfonden). JS was supported by ERC Project No. 267117 (DARK) hosted by Université Pierre et Marie Curie (UPMC) - Paris 6.

* Electronic address: msahlen@msahlen.net

- [1] D. Rapetti, C. Blake, S. W. Allen, A. Mantz, D. Parkinson, and F. Beutler, *MNRAS* **432**, 973 (2013), 1205.4679.
- [2] L. Xu, *PRD* **88**, 084032 (2013), 1306.2683.
- [3] A. Pisani, P. M. Sutter, N. Hamaus, E. Alizadeh, R. Biswas, B. D. Wandelt, and C. M. Hirata, *PRD* **92**, 083531 (2015), 1503.07690.
- [4] S. W. Allen, A. E. Evrard, and A. B. Mantz, *ARAA* **49**, 409 (2011), 1103.4829.
- [5] T. Y. Lam, J. Clampitt, Y.-C. Cai, and B. Li, *MNRAS* **450**, 3319 (2015), 1408.5338.
- [6] J. Brandbyge, S. Hannestad, T. Haugbølle, and Y. Y. Y. Wong, *JCAP* **9**, 014 (2010), 1004.4105.
- [7] E. Massara, F. Villaescusa-Navarro, M. Viel, and P. M. Sutter, *JCAP* **11**, 018 (2015), 1506.03088.
- [8] S. Chongchitnan and J. Silk, *ApJ* **724**, 285 (2010), 1007.1230.
- [9] M. Sahlén, Í. Zubeldía, and J. Silk, *ApJL* **820**, L7 (2016), 1511.04075.
- [10] R. Laureijs, J. Amiaux, S. Arduini, J. . Auguères, J. Brinchmann, R. Cole, M. Cropper, C. Dabin, L. Duvet, A. Ealet, et al., *ArXiv e-prints* (2011), 1110.3193.
- [11] R. S. de Jong, S. Barden, O. Bellido-Tirado, J. Brynnel, C. Chiappini, . Depagne, R. Haynes, D. Johl, D. P. Phillips, O. Schnurr, et al., *4most: 4-metre multi-object spectroscopic telescope* (2014), URL <http://dx.doi.org/10.1117/12.2055826>.
- [12] B. Sartoris, A. Biviano, C. Fedeli, J. G. Bartlett, S. Borgani, M. Costanzi, C. Giocoli, L. Moscardini, J. Weller, B. Ascaso, et al., *MNRAS* **459**, 1764 (2016), 1505.02165.
- [13] L. Amendola, S. Appleby, A. Avgoustidis, D. Bacon, T. Baker, M. Baldi, N. Bartolo, A. Blanchard, C. Bonvin, S. Borgani, et al., *ArXiv e-prints* (2016), 1606.00180.
- [14] 4MOST Consortium, in prep.
- [15] M. Sahlén, P. T. P. Viana, A. R. Liddle, A. K. Romer, M. Davidson, M. Hosmer, E. Lloyd-Davies, K. Sabirli, C. A. Collins, P. E. Freeman, et al., *MNRAS* **397**, 577 (2009), 0802.4462.
- [16] E. V. Linder, *PRD* **72**, 043529 (2005), astro-ph/0507263.
- [17] W. A. Watson, I. T. Iliev, A. D'Aloisio, A. Knebe, P. R. Shapiro, and G. Yepes, *MNRAS* **433**, 1230 (2013), 1212.0095.
- [18] W. Hu and A. V. Kravtsov, *ApJ* **584**, 702 (2003), astro-ph/0203169.
- [19] R. K. Sheth and R. van de Weygaert, *MNRAS* **350**, 517 (2004), astro-ph/0311260.
- [20] E. Jennings, Y. Li, and W. Hu, *MNRAS* **434**, 2167 (2013), 1304.6087.
- [21] F. Leclercq, J. Jasche, P. M. Sutter, N. Hamaus, and B. Wandelt, *JCAP* **3**, 047 (2015), 1410.0355.
- [22] U. Seljak and M. Zaldarriaga, *ApJ* **469**, 437 (1996), astro-ph/9603033.
- [23] S. Nadathur, *MNRAS* **461**, 358 (2016), 1602.04752.
- [24] P. M. Sutter, G. Lavaux, B. D. Wandelt, D. H. Weinberg, M. S. Warren, and A. Pisani, *MNRAS* **442**, 3127 (2014), 1310.7155.